Hole Injection Sequence in $BaCuO_2$ as Seen by XANES

Norberto Morgante, Paolo Ghigna[a], and Giorgio Spinolo[a]

Dipartimento di Scienza dei Materiali, Università di Milano-Bicocca, Via Emanueli 15, I-20122 Milano

[a] Dipartimento di Chimica Fisica, Università di Pavia, Viale Taramelli 16, I-27100 Pavia

Reprint requests to Dr. P. G.; e-mail: paolo@chifis.unipv.it, Fax: +390382507575

Z. Naturforsch. **55a,** 467–472 (2000); received December 27, 1999

Cu-L_{III} XANES data collected on $Ba_{0.98}CuO_{1.98+\delta}$ samples with different oxygen content are reported. The near-edge structures are discussed together with previous conductivity measurements, and an estimate of the hole density evolution with oxygen doping is given. The reported results give evidence of the increase with δ of the localization of doping holes on oxygen atoms.

1. Introduction

$BaCuO_2$ is the key compound in the solid state synthesis of $YBa_2Cu_3O_{7-\delta}$ superconductor [1, 2]. The complete crystal structure of barium cuprate (space group $Im\bar{3}m$, $a = 18.3$ Å) has been reported fairly recently [3]. It is capable of accommodating a large amount of oxygen atoms beyond the stoichiometric composition (up to 10% of the stoichiometric coefficient [4]). This makes $BaCuO_2$ an interesting system from the point of view of defect chemistry. Previous works have been carried out by means of oxygen non-stoichiometry determinations [4], conductivity, and thermopower measurements [5], the latter having shown that holes give the major contribution to conductivity. Conductivity data, however, have provided no conclusive arguments in favour of any particular model for defect equilibria. With regards to this issue, XANES (X-ray Absorption Near Edge Structure) is to be considered a particularly valuable tool, since it is able to probe the density of states associated with doping holes, i.e. it can yield direct information on the carrier density.

The Cu-L_{III} XANES white line lays at ≈931 eV and, in the case of hole doped cuprates, it exhibits a so-called *high energy tail* due to a weak absorption peak laying at ca. 933 eV. Following early assignments by Bianconi et al. [6], the main line is associated with the dipole allowed transition

$$|3d^9\rangle \rightarrow |\underline{2p}_{3/2}\, 3d^{10}\rangle \qquad (1)$$

(where $\underline{2p}_{3/2}$ indicates the core hole following photoabsorption); while the smaller peak at higher energy is to be attributed to the transition

$$|3d^9\,\underline{L}\rangle \rightarrow |\underline{2p}_{3/2}\, 3d^{10}\,\underline{L}\rangle, \qquad (2)$$

where $\underline{L}$ indicates an O-2p covalent hole. It may be worth noting here that cuprates, being properly described as charge-transfer systems [7, 8], $3d^9\,\underline{L}$ states correspond within a band structure approach to hole states in the valence band.

Formally, Cu(II) ions is described by an admixture of configurations $|3d^9\rangle$ and $|3d^{10}\,\underline{L}\rangle$ (i.e. by $\alpha|3d^9\rangle + \beta|3d^{10}\,\underline{L}\rangle$, with $\alpha^2 + \beta^2 = 1$). Wide experimental evidence [9–13] has led to the conclusion that the character of doping states in cuprates is mainly O-2 p. Thus, doping hole states are associated with the configuration admixture $\alpha'|3d^9\,\underline{L}\rangle + \beta'|3d^{10}\,\underline{L}^2\rangle$. Because of dipole selection rules, only configurations $|3d^9\rangle$ and $|3d^9\,\underline{L}\rangle$ can be reached by Cu-L_{III} XANES. The densities of Cu(II) and Cu(III) can be measured by the spectral weight of transitions with $|3d^9\rangle$ and $|3d^{19}\,\underline{L}\rangle$ initial states, respectively, if the assumption $\alpha = \alpha'$ is made. Such an assumption implies the neglect of both core-hole effects and spectral weight transfer. Several experimental evidences [14, 22, and references therein] allow one to state that it holds to a first approximation. Within this assumption, the actual density of itinerant doping holes (as it has first been suggested by Merrien et al. [15]) is given by

$$[h^\bullet] = A_2/(A_1 + A_2), \qquad (3)$$

once A_1 and A_2 have been assigned to the areas of the main line and of the high energy peak, respectively.

The quantitative interpretation of Cu-L_{III} XANES is still an open problem regarding both the description of

0932-0784 / 00 / 0300-0467 $ 06.00

single particle excitations and the determination of the exact character of doping hole states in cuprates. Making progress in these directions appears as a fundamental step in understanding the occurrence of superconductivity in these systems. In that view, systematic XANES studies on cuprates with various oxygen doping are highly valuable.

In the present work we report and discuss Cu-L_{III} XANES data on samples with different oxygen content in order to shed light on the hole injection sequence induced by doping in $BaCuO_2$.

2. Experimental

2.1 Materials

Previous works by our group [4, 5] have indicated that "$BaCuO_2$" is monophasic for oxygen partial pressures ranging from 10^{-5} to 1 atm, provided Ba:Cu = 88:90 ($\approx$ 0.98:1).

Compounds with this cation molecularity ($Ba_{0.98}CuO_{1.98+\delta}$) have been synthesized by solid state reaction from BaO_2 and CuO powders (Fluka *puriss.*) [4].

Three samples with different oxygen stoichiometries have been obtained by annealing under well controlled external conditions and subsequent fast quenching down to room temperatures. Samples A, B, C have been annealed for two days at 730 °C and $p(O_2) = 10^{-3}$ atm, 720 °C and $p(O_2) = 1$ atm, and 360 °C and $p(O_2) = 1$ atm, respectively, leading to a precisely known oxygen content (δ = 0.08, 0.14 and 0.20, respectively). The dependence of δ on T and $p(O_2)$ has been fully investigated and reported in [4].

2.2 Methods

Cu-L_{III} XANES spectra have been collected at beam line 3.4 at the Daresbury Synchrotron Radiation Source (Warrington, UK), employing an order sorting monochromator with a double Be ($10\underline{1}0$) crystal ($2d$ = 15.954 Å), the ring current ranging from 100 to 200 mA. Total electron yield has been used as detection technique, which probes ca. 200 Å depth at these energies and in this kind of systems [16]. Samples ($w \approx 40$ mg) have been mixed with ultra-pure graphite in an agate mortar and pressed to pellets. The experimental chamber has been kept under high vacuum. All spectra have been collected at room temperature. The experimental reproducibility was controlled performing two scans on each sample.

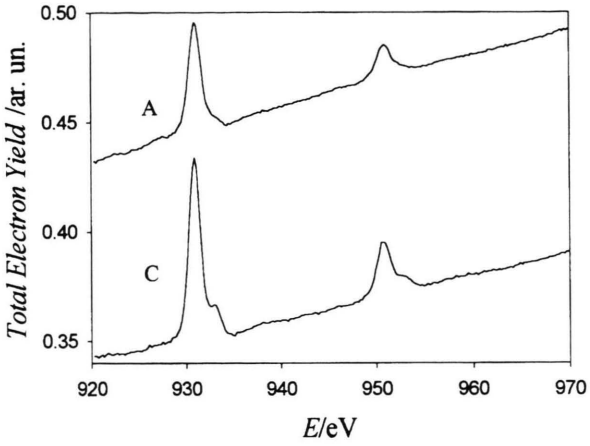

Fig. 1. Cu-L_{III} edge XAS in $Ba_{0.98}CuO_{1.98}$. Samples with lowest (A) and highest (C) oxygen content.

$BaCuO_2$ is known to be sensitive to CO_2 and H_2O. In order to check on the occurrence of any relevant chemical modification, data have been collected on the same samples and in the same beam line four months later. A very good reproducibility was assessed.

Each absorption line has been fitted, employing a pseudo-Voigt function, in order to account for both intrinsic and experimental broadening, which shows Lorentzian and Gaussian shape, respectively. The fit has been performed using a MINUIT routine [17], the fitting parameters being: energy position, area, width and Lorentzian/Gaussian character; see [18] for further details.

3. Results

Figure 1 displays the absorption spectra resulting from the addition of the two scans performed on each of samples A and C (those with lowest and highest oxygen content, respectively). Their main features are the resonance structures associated with Cu-L_{III} and Cu-L_{II} edges laying at ca. 931 eV and 951 eV, respectively, the latter showing significantly lower intensity.

The signal due to transition (2) can be clearly seen at ca. 933 eV, especially in the lower spectrum of Figure 1. It is worth noting that this transition appears with a higher energy resolution than it does for superconducting cuprates. This is possibly associated with the peculiar structure of $BaCuO_2$: since it can be seen as the result of the arrangement of quasi-molecular atomic clusters, the band structure could be described as the result of a weak

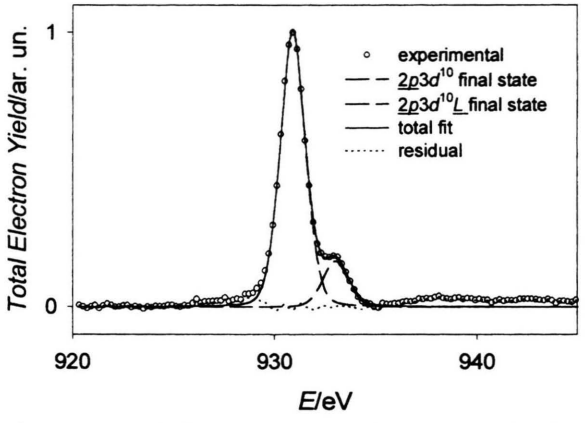

Fig. 2. Sample C: fit on background-subtrated Cu-L_{III} XAS.

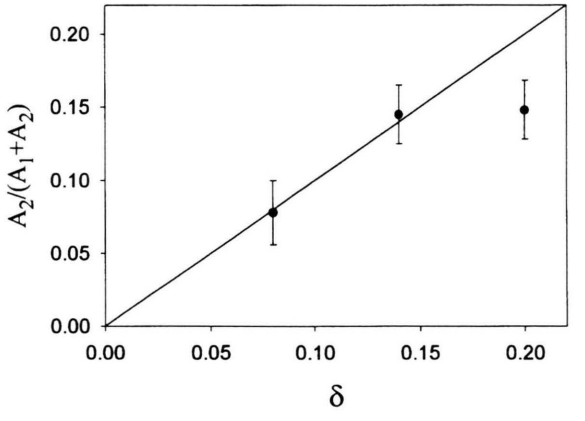

Fig. 3. Itinerant doping hole density measured as $A_2/(A_1 + A_2)$ vs. oxygen content δ.

overlapping of pseudo-molecular orbitals; reasonably enough, such bands can be expected to be narrower than the corresponding bands in perovskite cuprates, thus leading to narrower resonance lines.

Extraction of the background signal has been found somewhat complicated due to the weak features in the region 922–929 eV. Similar features have also been recently found in Cu-L_{III} spectra collected on BISCCO superconducting cuprate [19], and are also evident in spectra of other superconducting cuprates reported in the literature [20, 21, 22]. Their intensity does not seem to be related to the oxygen content. They rather can be explained as a surface effect enhanced by the specific sensitivity of the total electron yield method, since they appear to increase with the amount of time the sample has spent in the experimental chamber. The background

Table 1. Energy positions for absorption signals due to transitions to $3d^{10}\underline{L}$ and $3d^9\underline{L}$ final states (E_1 and E_2, respectively) and calculated resonance areas (A_1 and A_2, in arbitrary units). The doping hole density [h•] is measured by the ratio $A_2/(A_1 + A_2)$, while δ measures the oxygen overstoichiometry.

Sample	E_1/eV	E_2/eV	A_1	A_2	[h•]	δ
A	930.95	932.9	1.76	0.15	0.08	0.08
B	930.85	932.9	1.63	0.27	0.14	0.14
C	930.9	932.95	1.64	0.29	0.15	0.20

has been modelled by means of a polynomial curve fitting the pre-edge region below 926 eV and the energy region 940–945 eV, also accounting for the absorption jump, which has been found to be about one 50th of the maximum in the background subtracted absorption signal. The above mentioned anomalous features have been excluded in order to perform a physically meaningful background subtraction. In all cases, coefficients associated with terms higher than 1st order have been refined to values close to zero, i.e., the background could be modelled by nearly straight lines. The widths of the pseudo-Voigt used to fit each spectrum have been constrained to be equal during the fitting procedure. All fitted lines have been found to be mainly Gaussian, the amount of the Gaussian component varying within a narrow range. Figure 2 displays the fitting curves together with the experimental data of the sample with the highest oxygen content.

Experimental values for $A_2/(A_1 + A_2)$ are listed in Table 1 and displayed as a function of δ in Figure 3. Error bars in Fig. 3 extend beyond the statistical error on single spectra and have been estimated on the basis of the comparison between two sets of experimental data collected with a time interval of four months.

4. Discussion

The first and second experimental values of [h•] (given by $A_2/(A_1 + A_2)$) lay well inside the errors on a straight line with unit slope crossing the origin. Since the origin represents a situation where there are no extrinsic electronic defects, the linear trend strongly suggests the existence of a homogeneous behaviour for $0 < \delta < 0.14$. No experimental data at room temperature are available for $\delta < 0.08$, because of the difficulty of performing an efficient quenching at the required external conditions. The presence of a linear trend with unit slope indicates the formation of a single hole per each additional oxygen atom. In view of the fact that in $BaCuO_2$ no electronic

states other than Cu-3d and O-2p lay close to the Fermi energy E_F we must conclude that the formation of only one hole per oxygen doping atom is due to partial localization of holes in O-2p states, which do not mix with Cu-3d states, consequently being invisible to Cu-L_{III} XAS because of the dipole selection rules.

On the other side ($\delta > 0.14$), it is apparent from Fig. 3 that a saturation effect in [h•] vs. δ takes place. This saturation effect is to be considered as a fully reasonable result. Indeed, when a large amount of oxygen atoms is introduced by doping, it has to be expected that any further oxygen atom will be accommodated in a low Madelung-potential region: p-states associated with such atoms will certainly lay at higher energies, with consequent lower ability of producing holes in the valence band.

The above results agree with a band-structure model in which valence electronic states introduced by doping lay at energies close to the upper edge of the valence band when $\delta < 0.14$. Electronic states introduced when $\delta > 0.14$ are at higher energies. The overall understanding corresponds to the schematic energy-band diagram in Figure 4. Therefore, two different types of hole states are produced by doping: (i) itinerant holes in the valence band with a mixed O-2p and Cu-3d character and (ii) localized holes having O-2p character.

Starting from the present XANES results it is possible to re-discuss conductivity data reported in [5]. Within the quasichemical defect treatment, the hole localization on O-2p states when $\delta \leq 0.14$ can be interpreted in terms of mono-ionized oxygen interstitials. Therefore, the pertinent quasichemical equilibrium can be written as

$$1/2\ O_2 \rightleftarrows O_i' + h^\bullet, \tag{4}$$

the corresponding equilibrium constant being

$$K = \frac{[h^\bullet][O_i']}{p(O_2)^{1/2}}, \tag{5}$$

if variations in the number of available sites for the interstitials are neglected. Moreover, when intrinsic ionization does not occur,

$$[h^\bullet] = [O_i'], \tag{6}$$

and it is possible to obtain the simple relation

$$\log [h^\bullet] = \log K + 1/4 \log p(O_2), \tag{7}$$

which can be used to analyze experimental conductivity data, since the conductivity (σ) can be expressed as

$$\sigma = \mu e [h^\bullet], \tag{8}$$

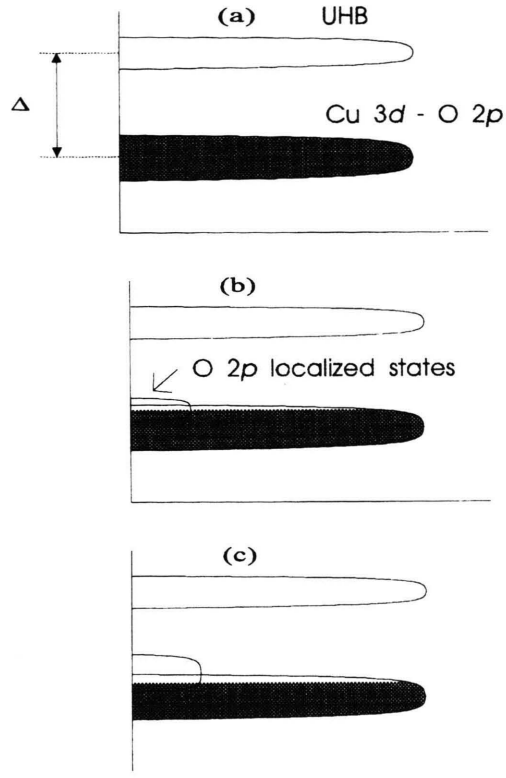

Fig. 4. Energy band diagram as a function of doping. Panels correspond qualitatively to: (a) $\delta = 0$; (b) indermediate δ values; and (c) high δ values. Δ denotes the charge-transfer energy.

where e denotes the electron charge. Assuming that the carrier mobility (μ) depends only on the temperature, one obtains:

$$\log \sigma \propto 1/4 \log p(O_2). \tag{9}$$

Thus, a linear dependence with 1/4 slope for $\log \sigma$ as a function of $\log p(O_2)$ should be observed whenever the equilibrium (4) is dominant. According to our XANES results, this should occur when $\delta \leq 0.14$. In Fig. 5 experimental conductivity data are displayed together with straight lines with 1/4 slope.

On the basis of the previous discussion it is now possible to qualitatively explain the conductivity data. First of all, Fig. 5 shows that at very low δ-value (i.e. at high temperature and low oxygen partial pressure) the conductivity data exhibit a slope significantly lower than expected on the basis of the quasichemical treatment (9). In our opinion, this lower slope is due to the failure of assumption (6): a significant amount of holes and elec-

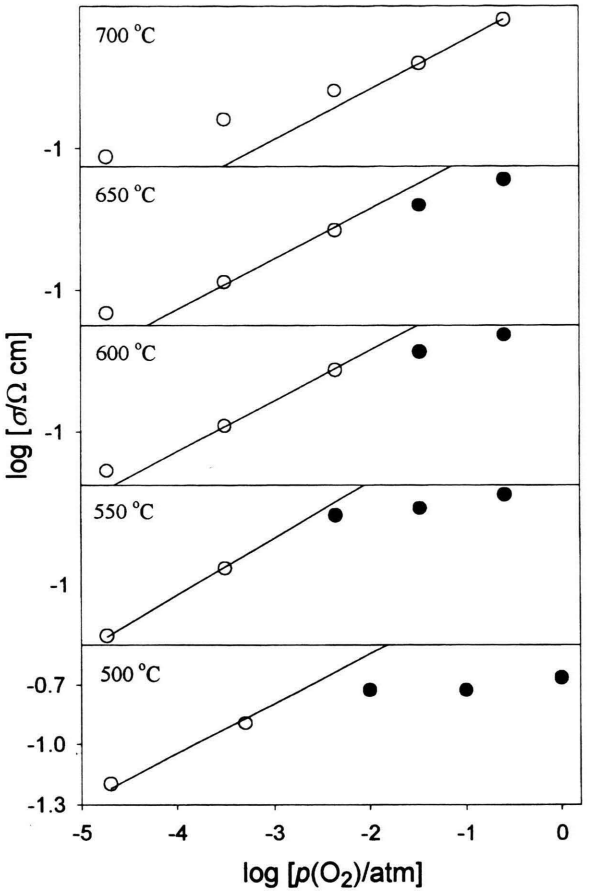

Fig. 5. Conductivity as a function of oxygen partial pressure. Data corresponding to different temperatures. Empty circles: $\delta \leq 0.14$; filled circles: all other data.

trons is produced by thermal excitation across the band gap at the high temperatures where the conductivity measurements have been made. Therefore the amount of holes is higher than predicted by (6), and the difference is the higher the lower is δ. In addition, excited electrons also contribute to the conductivity. The influence of intrinsic ionization is not seen by these XANES data, since the measurements have been made at room temperature.

In an intermediate range of the oxygen partial pressure, which depends on temperature and roughly corresponds to $\delta = 0.12$, the behaviour implied by (9) is closely obeyed. This means that oxygen doping buffers intrinsic ionization at this larger δ values. It is worth remarking here that the hypothesis of the formation of doubly ionized interstitial oxygen atoms would lead to the expectation of a 1/6 slope, which could not explain the conductivity data in this range.

Finally, for $\delta > 0.14$, a saturation behaviour is apparant in the trend of σ vs. $p(O_2)$. This can be related to the saturation of δ with respect to $p(O_2)$ (an effect which is directly shown by oxygen non-stoichiometry data [4]) and to the saturation behaviour of [h$^\bullet$] vs. δ (as shown by our XANES data, Figure 3).

5. Conclusions

The present work report on the analysis of Cu-L_{III} XANES data in $BaCuO_{2+\delta}$ as a function of δ. XANES results point towards a non linear relation between δ and the itinerant hole density, which saturates with respect to the oxygen doping for $\delta > 0.14$. The analysis of the XANES data together with previous conductivity measurements suggests that oxygen sites have a significant spread in energy: the lower laying sites are filled first (at lower δ) and give rise to mono-ionized interstitials, the higher energy sites are filled at larger over-stoichiometries and preferentially produce union-ized interstitials, i.e., doping holes tend to be fully localized on O-2p states.

Acknowledgements

This work has been partially supported by the Department of University and Scientific and Technological Research of the Italian Government (MURST 40%) and by a grant from Daresbury laboratory for the provision of beam time, and it is based on a thesis submitted by one of the authors (N.M.) in fulfillment of the requirements for the Laurea degree in Chemistry at the Università di Pavia.

[1] G. Flor, M. Scavini, U. Anselmi-Tamburini, and G. Spinolo, Solid State Ionics **43,** 77 (1990).
[2] U. Anselmi-Tamburini, P. Ghigna, G. Spinolo, and G. Flor, J. Phys. Chem. Solids **52,** 715 (1991).
[3] E. F. Paulus, G. Wlschek, and H. Fuess, Z. Kristallographie **209,** 586 (1994).
[4] G. Spinolo, U. Anselmi-Tamburini, M. Arimondi, P. Ghigna, and G. Flor, Z. Naturforsch. **50a,** 1050 (1995).
[5] G. Chiodelli, U. Anselmi-Tamburini, M. Arimondi, G. Spinolo, and G. Flor, Z. Naturforsch. **50a,** 1059 (1995).
[6] A. Bianconi, A. Congiu Castellano, M. De Santis, P. Rudolf, P. Lagarde, and A. M. Flank, Solid State Commun. **63,** 1009 (1987).
[7] A. Fujimori, F. Minami, and S. Sugano, Phys. Rev. B **29,** 5225 (1984).

[8] G. A. Sawatzky and G. W. Allen, Phys. Rev. Lett. **53,** 2239 (1984).
[9] A. Bianconi, A. Clozza, A. Congiu-Castellano, S. Della Longa, M. De Santis, A. Di Cicco, K. Garg, P. Delogu, A. Gargano, R. Giorgi, P. Lagarde, A. M. Flank, and A. Marcelli, Int. J. Mod. Phys. **B1**, 853 (1987).
[10] A. Bianconi, A. Congiu Castellano, M. De Santis, P. Delogu, A. Gargano, and R. Giorgi, Solid State Commun. **63,** 1135 (1987).
[11] A. Bianconi, J. Budnick, A. M. Flank, A. Fontaine, P. Lagarde, A. Marcelli, H. Tolentino, B. Chamberland, C. Michel, B. Raveau, and G. Demazeau, Phys. Lett. A **127,** 285 (1988).
[12] T. Mizokawa, H. Namatame, A. Fujimori, K. Akeyama, H. Kondoh, H. Kuroda, and N. Kosugi, Phys. Rev. Lett. **67,** 1638 (1991).
[13] N. Merrien, F. Studer, C. Michel, P. Srivastava, B. R. Sekhar, N. L. Saini, K. B. Garg, and G. Tourillon, J. Phys. Chem. Solids **54,** 499 (1993).
[14] F. Studer, C. Gasser, L. Coudrier, H. Murray, M. Pompa, A. M. Flank, and P. Lagarde, Physica B **208–209,** 521 (1995) and references therein.
[15] N. Merrien, F. Studer, G. Poullain, C. Michel, A. M. Flank, P. Lagarde, and A. Fontaine, J. Solid State Chem. **105,** 112 (1993).
[16] M. Pompa, P. Castrucci, C. Li, U. Udron, A. M. Flank, P. Lagarde, H. Katayama-Yoshida, S. Della Longa, and A. Bianconi, Physica C **184,** 102 (1991).
[17] F. James and M. Ross, CERN Computer Centre Program Library, Program D506.
[18] P. Ghigna, G. Spinolo, M. Scavini, U. Anselmi-Tamburini, and A. V. Chadwick, Physica C **253,** 147 (1995).
[19] P. Ghigna, G. Spinolo, G. Flor, and N. Morgante, Phys. Rev. B **57,** 13426 (1998).
[20] A. Q. Pham, F. Studer, N. Merrien, A. Maignan, C. Michel, and B. Raveau, Phys. Rev. B **48**, 1249 (1993).
[21] N. Merrien, L. Coudrier, C. Martin, A. Maignan, and F. Studer, Phys. Rev. B **49,** 9906 (1994).
[22] F. Studer, in X-Ray Absorpt. Bulk Surf., K. Garg, E. A. Stern, and D. Norman, Eds., World Science Publ., Singapore 1994.